JOURNAL OF PROPULSION AND POWER
Vol. 9, No. 1, Jan.–Feb. 1993

Scramjet Fuel-Air Mixing Establishment in a Pulse Facility

R. Clayton Rogers* and Elizabeth H. Weidner†
NASA Langley Research Center, Hampton, Virginia 23665

A numerical simulation of the temporally developing flow through a generic scramjet combustor duct is presented for stagnation conditions typical of flight at Mach 13. The particular focus is to examine the startup transients and to determine the time required for certain flow parameters to become established. The calculations were made with a Navier-Stokes solver SPARK with temporally relaxing inflow conditions derived from the operation of the T4 shock tunnel at the University of Queensland in Australia. The generic combustor geometry includes the injection of hydrogen fuel from the base of a centrally located strut. The flow was assumed laminar and fuel combustion was not included. The establishment process is presented for viscous parameters in the boundary layer and for parameters related to the fuel-air mixing.

Nomenclature

C_f = skin friction coefficient
$\overline{C_f}$ = normalized C_f in transient flow case, $C_f\sqrt{Re}$
C_h = Stanton number
$\overline{C_h}$ = normalized C_h in transient flow case, $C_h\sqrt{Re}$
f = fuel mass fraction
f_R = fuel mass fraction that is reactable
G_s = characteristic flow time
k = thermal conductivity
L_c = characteristic length
M = Mach number
$\dot{m}_R$ = mass flow ratio
P = static pressure
Pr = Prandtl number
P_s = stagnation or nozzle supply pressure
Re = Reynolds number
T = temperature
T_{aw} = adiabatic wall temperature
t = time
U_c = characteristic velocity
u = local velocity
x, y = longitudinal and transverse coordinates
y_w = location of upper wall boundary, 0.02357 m
δ = boundary-layer thickness
δ^* = displacement thickness
η_m = mixing efficiency parameter
θ = momentum thickness
ρ = mass density
τ_e = establishment time
ϕ = fuel equivalence ratio

Subscripts
e = boundary-layer edge conditions
in = inflow plane conditions
N = normalized values
w = wall values

Introduction

RESEARCH related to the operation of a scramjet engine at conditions corresponding to flight at speeds above Mach 8 have been underway at both government and university laboratories. The high stagnation energy of the flow required to simulate these conditions exceeds that which can be readily obtained from ground facilities in which the test gas is heated by an electric arc or by combustion. The test facility of choice has been a shock tube that heats the test medium by the passage of a strong shock wave. Test facilities of this type (called reflected shock tunnels) at the Australian National University (named T3) and the University of Queensland (named T4) in Australia have led in the experimental testing and study of fuel-air mixing and combustion phenomena in a scramjet at hypervelocity conditions. A recent review of these facilities[1] and typical examples of the experimental research[2,3] have been presented.

With the renewed interest in transatmospheric flight, other facilities capable of producing test gas flows at energy levels typical of hypervelocity flight have been constructed. Two such facilities are NASA's HYPULSE Facility at the General Applied Science Laboratories in New York[4,5] and the free-piston-driven reflected shock tunnel T5 at GALCIT at the California Institute of Technology.[6] Although capable of supplying a test gas with the stagnation enthalpy level of hypervelocity flight, these pulse facilities generally lack the stagnation pressure needed for a full simulation at flight altitude. However, for scramjet combustor research, the expansion of the shock tunnel flow is used to produce a short pulse of test gas at conditions typical of those expected at the entrance to a scramjet combustor. In addition to the short test time (on the order of a millisecond) the flow may be transient throughout the useful test period between the flow establishment and the arrival of driver gases. The short test times are of concern when doing mixing and combustion experiments related to scramjets because of the time required for certain important flow processes to become established or to reach a stable condition. In addition, the possibly transient flow may delay the approach of certain flow parameters to a quasisteady state.

In a previous study[7] the flow from a shock tunnel through a generic scramjet combustor was numerically modeled for cases with steady and transient inflow. The focus of that study was to examine time-accurate numerical simulations of the facility flow through the scramjet combustor duct and assess the time required for certain parameters to become established. Among these parameters were the size of the recirculation zone formed at the base of a fuel injector strut (without fuel injection), boundary-layer thicknesses, shear stress along the duct wall, and the heat flux to the cold wall.

The goal of the current work is to include the effect of fuel injection from the strut base on both the flow starting process and the approach to a stable or quasisteady (if transient flow) condition. For the conditions corresponding to Mach 13 flight enthalpy, this flow was examined by the assumption that the

Received Jan. 4, 1991; presented as Paper 91-0229 at the AIAA 29th Aerospace Sciences Meeting, Reno, NV, Jan. 7–10, 1991; revision received June 1, 1992; accepted for publication June 22, 1992.
*Senior Research Scientist. Member AIAA.
†Research Technologist.

condition of a parcel of fluid in transient flow may be related to a reference state at an earlier time, which is sometimes referred to as the hypersonic equivalency principle.[8]

Numerical Model and Analysis

Computational Model

The numerical simulation of the flow from a reflected shock tunnel (pulse facility) through a generic scramjet combustor was performed with the Navier-Stokes solver SPARK which has been previously applied to a range of supersonic mixing, combustion, and nozzle flows.[9–11] This computer code solves the full Navier-Stokes equations and the conservation equations for energy, mass, and species for the mixing of hydrogen fuel with air. The calculations were made assuming laminar flow and without combustion of the fuel; both turbulence and chemical reaction will be included in subsequent studies. Turbulence was excluded because of the added numerical complexity involved in modeling the transition from laminar flow during the flow startup process, particularly with transient inflow. The code was run in a time-accurate manner on a Cray Y-MP supercomputer.

Combustor Geometry

The geometry of the two-dimensional combustor duct modeled in this study is presented in Fig. 1. The hydrogen fuel was injected parallel to the airflow from a Mach 3.3 nozzle that effectively covered the base of the central strut. In applying the SPARK code to the duct flow, only the top half of the duct was considered and the portion of the strut that extends upstream of the duct entrance plane was neglected. Thus, the computational domain was two-dimensional with a rearward-facing step representing the strut base. The center plane of the duct was assumed to be a plane of symmetry. The computational domain was discretized over a mesh with 288 by 86 grid points in the x- and y-coordinate directions, respectively, and was highly compressed in regions near the wall boundaries and at the strut base where large gradients in the flow parameters were expected. Minimum grid spacings in the x-direction were 0.1 cm at the inflow plane, and 0.025 cm at the strut base. In the y-direction, the grid had minimum spacing of 0.005 cm at the upper and lower boundaries and at the top of the strut. As is usual in a numerical procedure, the grid nodes within the strut were reset to the starting conditions after each integration step. Additional details of the grid-stretching procedure used in these calculations may be found in Ref. 7; general details are in the paper by Roberts.[12]

Initial Conditions

Boundary conditions along the wall boundary (at $y = 2.357$ cm) were set to the usual no-slip velocity condition, zero gradients for the pressure and species, and fixed wall temperature of 300 K. Fuel injection was specified by values of pressure, temperature, and velocity over 0.45 cm of the 0.50-cm strut base to approximately include the finite thickness of the injector lip. The inflow conditions were modeled after those for a typical run of the T4 reflected shock tunnel when fitted with a Mach 5 contoured nozzle and operated for scramjet testing. For this mode of operation, the stagnation pressure of the shock tunnel decays with time from a peak value as shown in Fig. 2, so as to delay the arrival of the driver gas. Additional details of this mode of operation for scramjet testing is given in Ref. 7. The stagnation pressure (or nozzle plenum pressure) reaches a peak value of about 62 MPa and then decays in a generally exponential manner during the run time. This pressure history was fit with a cubic function during the rise time from incident shock arrival to the peak and a decaying exponential function from then on.

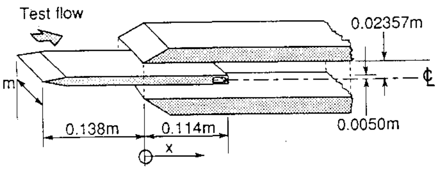

Fig. 1 Generic scramjet combustor duct geometry.

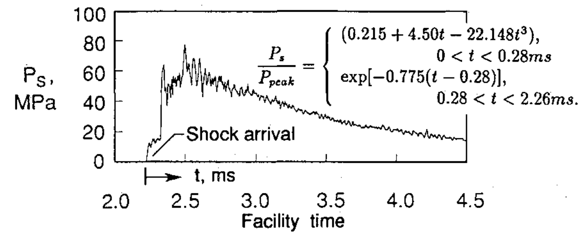

Fig. 2 Typical stagnation pressure history in T4 shock tunnel.

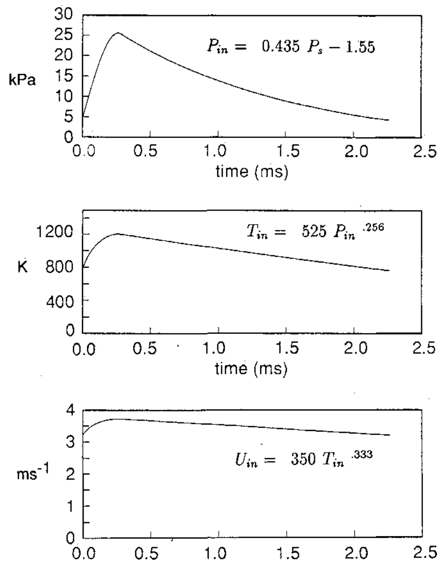

Fig. 3 Typical conditions at exit of T4 Mach 5 nozzle.

The conditions at the inflow of the combustor were obtained by expanding the nozzle plenum conditions through the nozzle area distribution using a one-dimensional real-gas code. The nozzle exit conditions, taken to be the same as the combustor entrance, were then fit with appropriate functions to obtain temporal variations given in Fig. 3. In Fig. 3, time zero is set to be the arrival of the test gas at the combustor duct entrance; the curves were used to specify the inflow conditions for the transient case. For the steady inflow case, nominal inflow conditions were a pressure of 21.5 kPa, temperature of 1165 K, and a velocity of 3670 m/s which correspond to the nominal stagnation pressure of 53 MPa at 0.5 ms after the incident shock arrival.

Injector Conditions

Injection of the hydrogen fuel from the strut base was specified by values of pressure, temperature, and velocity to give a stoichiometric fuel flow for the nominal steady airflow conditions. The injector exit conditions were determined assuming room temperature (300 K) hydrogen undergoing an isentropic expansion from the sonic throat to the exit area. The pressure, temperature, and velocity of the fuel injector exit were 5050 Pa, 94 K, and 2420 m/s, respectively.

In normal operation of the T4 shock tunnel, the fuel flow is started some 5 ms before the test gas flow, so that when the test gas arrives at the combustor duct entrance the duct is full of hydrogen and the fuel flow is at steady state. To simulate this operation for the numerically modeled flow starting process, a calculation was made with jet only. The computational boundary conditions at the duct entrance were designed to permit outflow of jet gas or entrainment of test cabin air. If the flow velocity was positive—indicating an inflow—then the pressure and temperature at the inflow plane were set to the initializing values of 300 Pa and 300 K, respectively, and the fuel mass fraction to zero. If the velocity was negative—indicating an outflow—then the pressure, temperature, and fuel mass fraction were held constant (zero gradient). After running for a sufficient time for the overall flow in the duct to reach steady state, these results were used to start the cases with steady and transient inflow air. Results from the calculation of the jet-only case are given in Fig. 4 and show the pressure field and hydrogen mass fraction field.

Computed Cases

Using these jet-only results to set the initial conditions in the combustor duct, the SPARK code was used to compute the flow through the combustor duct for two flow conditions: 1) a steady inflow at nominal conditions given previously; and 2) a transient inflow shown in Fig. 3. The calculations were made in a time-accurate manner for a total flow time of 1 ms. Because the hydrogen fuel that filled the duct at time-zero has a high sonic velocity (about twice that of the incoming air), the steep gradients between the inflow air shock front and existing velocity gradients in the hydrogen fuel plume caused some difficulty in obtaining a stable solution. In making these calculations the numerical stability factor (CFL number) was varied linearly from 0.1 to 0.8 over the first 18,000 time steps. Generally, the damping coefficients, which were based only on pressure, were set to 1.8 for all times. The exclusion of temperature from the damping terms permitted a more reliable representation of the thermal boundary layer for these cases with a cold wall, and therefore, of a heat flux parameter.

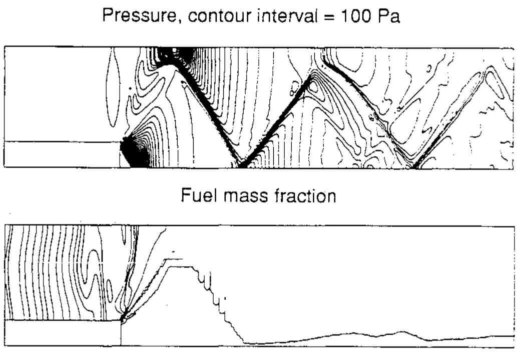

Fig. 4 Combustor conditions with jet only operating.

Procedures

The focus of this study was to examine the establishment process for mixing in a scramjet combustor for the impulsively started flow from a shock-tunnel facility. The following paragraphs will briefly present the concept of establishment and the procedure used in this article to define the establishment times of selected parameters. Before discussing this procedure it is helpful to observe the features of the flow development for the steady and transient inflow cases.

Flow Structure and Development

A comparison of the developing flow is shown in Fig. 5 for conditions of steady and transient inflow. For each case the pressure contours at intervals of 1000 Pa and contours of hydrogen mass fractions are given at the times indicated. For ease of visualization the vertical coordinate has been stretched by a factor of five in each of the contour plots. The shock front of the test gas interface with the hydrogen fuel is quite evident in the fuel plume and pressure contours. As the airflow continues through the duct, the shock structure becomes more established and after about 0.20 ms, the major features and shock train have been formed in both the steady and transient cases. The contours of hydrogen mass fraction depict the effect of the hot, high-speed air pulse on the development of the fuel plume. Once the air shock front passes the strut base, the lower density hydrogen is effectively blown off and

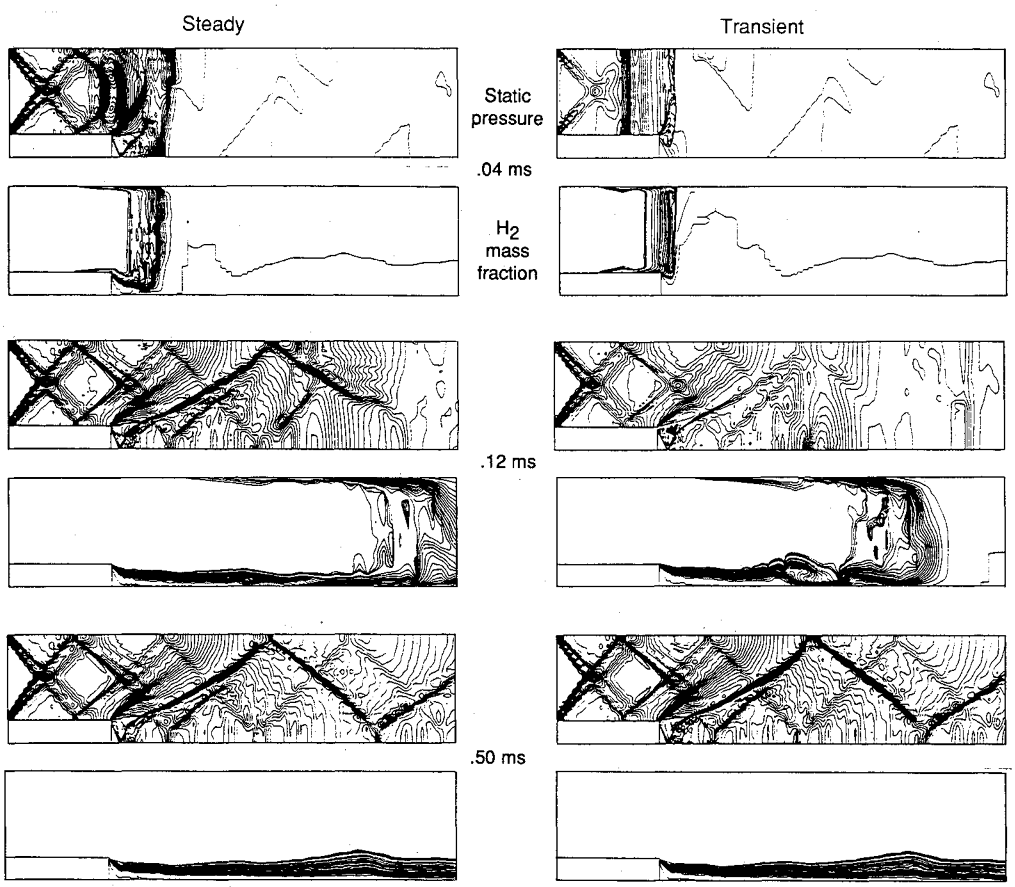

Fig. 5 Evolution of the pressure field and fuel plume for steady and transient inflow.

must be re-established. After sufficient flow time—approximately 0.20 ms—the structure of the fuel plume is established and remains nearly unchanged. Although calculations were made for a 1 ms flow time, results after 0.5 ms are not shown since no significant differences were evident.

It can be seen in these results that the transient case develops more slowly than the steady case as a result of the required rise time to the peak values. The average shock speeds were estimated to be approximately 4200 m/s upstream of the strut base and 4500 m/s downstream of the strut base for the steady inflow case. For the transient inflow case, the shock accelerated from about 2900–3200 m/s from the inflow plane to the strut base and reached an average speed of about 3800 m/s downstream of the strut when the hydrogen fuel plume was encountered.

Normalization for Transient Flow

An example of the overall flow establishment can be illustrated by the conservation of mass since it is an integral quantity of the flow. The air mass flow ratio $\dot{m}_R = \dot{m}_x/\dot{m}_{in}$ where $\dot{m}_x$ is the mass flow rate of air (per unit width of the duct) at location x, and $\dot{m}_{in} = \rho_{in}u_{in}\Delta y$ is the mass flow rate at the duct inflow of height Δy. The variation of this parameter as a function of time is presented in Fig. 6 for the steady and transient flow cases. For the transient inflow case, the mass inflow value was adjusted to account for the time delay between the inflow plane and the local x position, assuming a nominal flow velocity of 3670 m/s. This procedure,[8] in general, can be illustrated for a parameter q by the equation

$$\hat{q}(x, t) = \frac{q(x, t)}{q(x_{in}, t - \delta t)} \tag{1}$$

where the time delay is given as

$$\delta t = \frac{x - x_{in}}{U_{in}}$$

The application of this procedure provides a means of normalizing the flow parameters by following a parcel of flow downstream. For the mass flow ratios given in Fig. 6, the passage of the air shock is noted by the rapid rise in the mass flow. For the steady case, the mass flow is conserved and $\dot{m}_R$

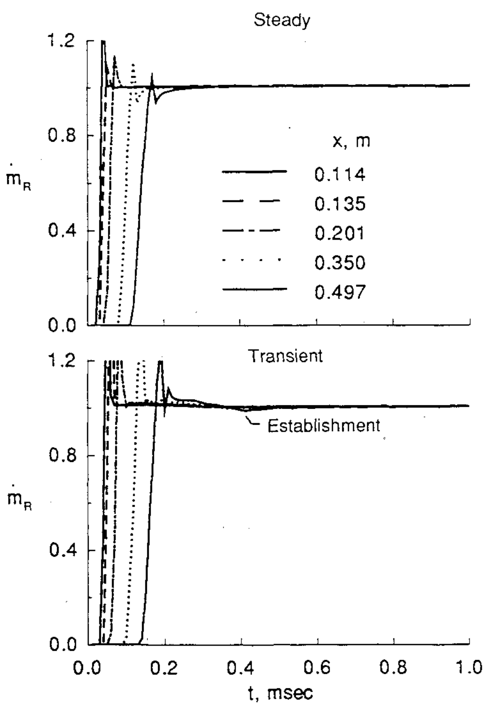

Fig. 6 Conservation of mass flow.

approaches a stable value of unity throughout the duct after about one passage of the flow through the domain. For the transient case, with the inflow value adjusted to the earlier time by the application of Eq. (1), the mass flow ratio also approaches unity and a stable or "established" value after about two flow passes. As an indicator of the overall flow establishment the mass flux ratio verifies the use of shifting to an earlier time to obtain quasisteady conditions throughout the flow.

The time taken for the flow parameter to approach an established (or stable) condition is represented by the characteristic flow time parameter

$$G_s = U_c\tau_e/L_c$$

where the establishment time τ_e is measured from the time of flow arrival. The U_c and L_c are characteristic values of the velocity and length. Typical values of this parameter are $G_s = 2$ for the boundary layer on a flat plate in laminar flow, and $G_s = 1$ for turbulent flow.[7] The establishment of the mass flow ratios (Fig. 6) corresponds to values of G_s of about 1.1 and 1.5 for the steady and transient cases, respectively.

Establishment Time

In the following paragraphs parameters are examined with regards to the time it takes to reach an established (or stable) value. For the steady inflow case, steady values were obtained by averaging the parameters over the time interval 0.8–0.95 ms. This interval provided for at least one flow pass through the duct. The maximum deviation of the parameter from this mean (steady) value was found within the averaging time interval and used to define the error band. An estimate of the establishment time was then found by searching backward in time until the parameter value was outside the error band. The error band was taken as twice the maximum deviation, with a minimum value of 2.5%. Visual examination of the parameter histories aided in the interpretation of the establishment time estimates.

For the transient inflow case, the parameters were (usually) normalized by the appropriate application of Eq. (1). However, the determination of a steady value was not usually possible and the parameters approached an asymptote late in the flow time. The onset of this near-linear variation was taken as indicative of the flow "establishment" for the transient case. In some cases, the parameters' histories were filtered over a time interval of 0.1 ms to eliminate periodic oscillations about an apparent mean. Examination of these filtered histories resulted in more consistent values of establishment times.

Results and Discussion

Boundary-Layer Parameters

The first indicators of flow establishment were those parameters dominated by the viscous layer near the wall. These "boundary-layer" parameters include the boundary-layer thickness, the displacement and momentum thicknesses, and the skin friction and heat flux. At each x-location the boundary-layer conditions were estimated by averaging over the 10 points just beyond the edge. The boundary-layer thickness was the location where the velocity was within 99% of the edge value. The displacement and momentum thicknesses were computed from the usual definitions. The temporal development of δ and δ^* on the wall at the strut base ($x = 0.114$ m) and the duct exit ($x = 0.497$ m) are given in Fig. 7 for the steady and transient inflow cases. The momentum thickness exhibited the same relaxation character as the displacement thickness. For the steady inflow case δ and δ^* achieve definite steady-state values. For the transient case δ and δ^* appear to reach "steady" values, particularly at the 0.114 m location, but exhibit an increasing trend at the duct exit position. Estimates of the establishment times for these param-

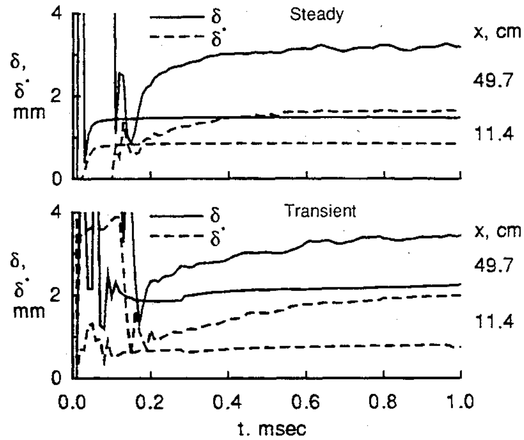

Fig. 7 Variation of boundary-layer thicknesses with time.

Table 1 Establishment times for boundary-layer parameters

Parameter		x-location, cm	
	11.4	20.1	49.7
C_f, s	0.21	0.28	0.61
t	0.47	0.52	0.70
C_h, s	0.19	0.17	0.61
t	0.47	0.43	0.71
δ, s	0.12	0.21	0.59
t	0.38	0.42	0.60
δ^*, s	0.13	0.20	0.58
t	0.39	0.47	0.62
θ, s	0.12	0.21	0.52
t	0.35	0.43	0.59

s = steady. t = transient.

eters are given in Table 1, where s and t refer to steady and transient cases, respectively.

The coefficient of skin friction and heat flux (Stanton number) are defined

$$C_f = \frac{\mu \left|\frac{\partial u}{\partial y}\right|_w}{\frac{1}{2}\rho_e u_e^2} \tag{2}$$

$$C_h = \frac{k \left|\frac{\partial T}{\partial y}\right|_w}{\rho_e u_e C_{pw}(T_{aw} - T_w)} \tag{3}$$

The thermal conductivity k was obtained from the definition of Prandtl number (taken to be 0.71), assuming air at the wall at 300 K to get values of specific heat and viscosity. These parameters are indicative of the friction and heat flux for the purposes of deducing flow establishment time issues, but because of insufficient numerical resolution of the velocity and temperature gradients at the wall, should not be taken as predictive values in the scramjet combustor flow. For the transient case, average conditions at the local boundary edge were adjusted to account for the flow delay by the application of Eq. (1).

The temporal development of these parameters is shown in Fig. 8 for the steady and transient inflow conditions at x locations of 0.114 and 0.497 m. For the steady inflow case, both parameters decay to steady values and C_h is about half of the C_f. For the transient inflow case (shown in the middle of Fig. 8) the parameters were computed by replacing the edge values with time varying density, velocity, and temperature values at the inflow, adjusted for the flow time delay. In spite of this adjustment C_f and C_h do not approach a steady

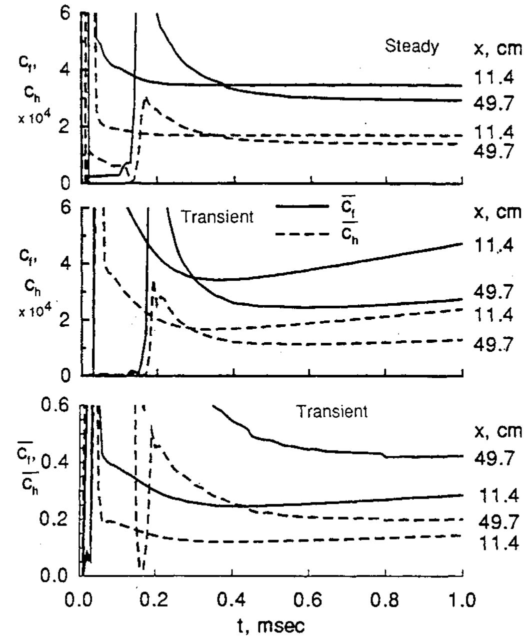

Fig. 8 Variation of skin friction and heat flux with time.

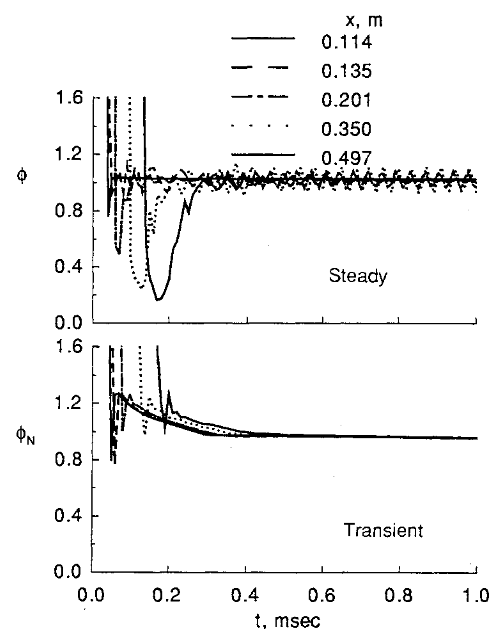

Fig. 9 Variation of equivalence ratio with time.

value but rather reach a minimum and then exhibit a fairly linear increase. Values of the estimated establishment times for these parameters were taken to be indicated by the point where the histories approached a linear variation and are given in Table 1. In another attempt to relate local values of C_f and C_h to some stable value in the transient flow, they were correlated with Reynolds number by defining parameters $\overline{C_f} = C_f\sqrt{Re_{in}}$ and $\overline{C_h} = C_h\sqrt{Re_{in}}$ where Re_{in} is the Reynolds number using inflow properties and based on the flow distance. These parameters are shown in the bottom part of Fig. 8 and indicate an improvement in the approach to quasisteady values. Estimates of the establishment times for these parameters were essentially the same as estimated for the local values (in the middle of Fig. 8).

Mixing Parameters

The approach of the hydrogen-fuel jet to an established condition was examined by the equivalence ratio and the accomplished mixing parameter. The variation of equivalence ratio with time is given in Fig. 9. For the steady inflow of fuel this parameter illustrates the approach of the overall flow to an established condition. Compared with the mass flow ratio in Fig. 6, the equivalence ratio includes the delay required to re-establish the fuel flow. For the steady case, ϕ at the exit plane (x = 0.5 m) approaches an established value after a characteristic time of about G_s = 1.8 (after flow arrival) compared with G_s = 1.1 for the mass flow. Referencing the establishment to the fuel jet, with exit velocity of 2.4 km/s, the characteristic time is about G_s = 1.3 after the flow arrives at the exit. This value is slightly greater than the mass flow time but warrants further examination to assess the full effect. For the transient case an equivalence ratio parameter was defined ($\phi_N = \phi/\phi_{\rm ref}$) as the local equivalence ratio referenced to the equivalence ratio $\phi_{\rm ref}$ based on the inflow air mass flow rate adjusted for the time delay by Eq. (1). Since the mass flow of fuel is steady, ϕ_N is the ratio of the overall mass flow (an inverse of $\dot{m}_R$), but includes the additional time needed for the fuel flow to become re-established.

The mixing efficiency parameter histories are shown in Fig. 10 for the steady and transient inflow cases. This parameter is defined as the fraction of total fuel at each location that could completely react. That is

$$\eta_m = \frac{\int \rho u f_R \, dy}{\int \rho u f \, dy}$$

where f is the mass fraction of fuel and f_R is the mass fraction that is reactable to completion. This reactable mass fraction is the local fuel mass fraction at points where the mixture is lean and is equal to the stoichiometric fraction where the mixture is fuel rich. The histories of the mixing parameter exhibit the effect of the starting shock and for the steady inflow case, reach establishment at progressively later times. The unsteadiness of η_m at the later time at x stations 20.1 and 35.1 cm is likely due to the shocks and expansions near these locations. Estimated establishment times for the steady flow case are given in Table 2.

For the transient inflow case, the mixing parameter reaches a maximum and then begins to decay in a nearly linear manner. The maximum at each location occurs about 0.3 ms after the arrival of the initial shock. This time delay is about the same as the rise time of the transient inflow conditions (see Fig. 2) when the mass flux is maximum. As with the other parameters, the establishment time for the transient flow was taken as the point at which the mixing parameter approached

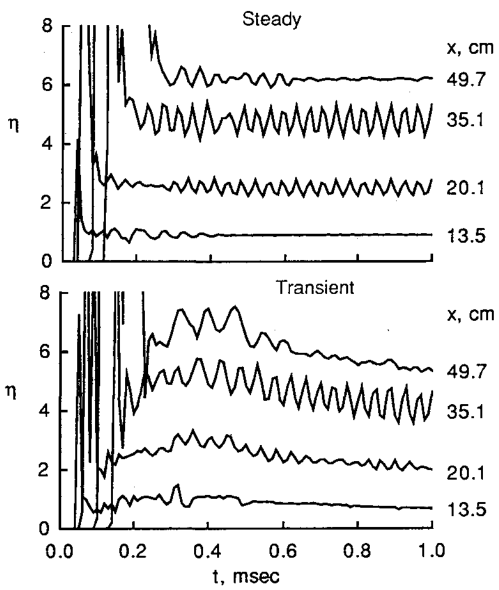

Fig. 10 Variation of fuel mixing efficiency with time.

Table 2 Establishment times for fuel mixing parameters

Parameter		x-location, cm 11.4	20.1	35.1	49.7
$y_{\rm edge}$,	s	0.25	0.21	0.34	0.38
	t	0.52	0.54	0.57	0.57
ϕ_R,	s	0.14	0.21	0.20	0.28
	t	0.51	0.54	0.60	0.68
η_m,	s	0.12	0.18	0.26	0.35
	t	0.54	0.56	0.60	0.66
λ,	s	0.06	0.09	0.15	0.21
	t	0.07	0.10	0.21	0.28

s = steady, t = transient.

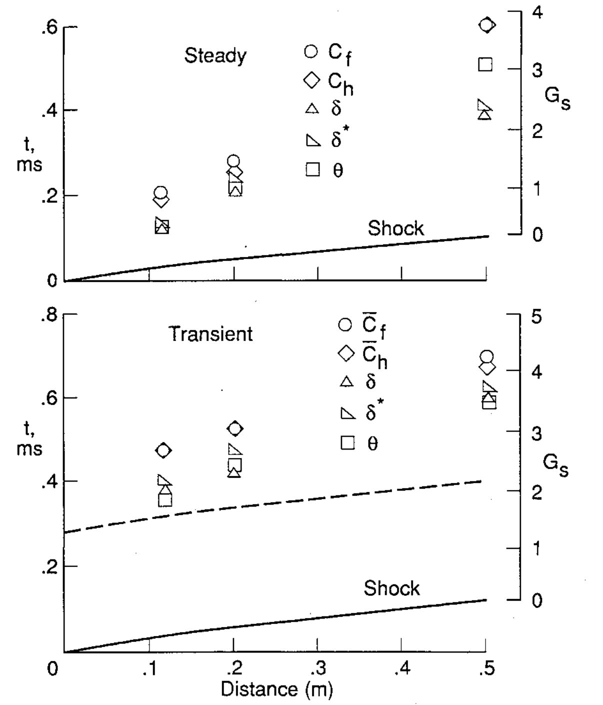

Fig. 11 Establishment times for boundary-layer parameters.

a constant (linear) decay rate. Estimated values of establishment times (in ms) are given in Table 2.

Flow Establishment

The estimates of establishment times as described above and listed in Tables 1 and 2 are plotted on an x-t diagram in Figs. 11 and 12. The path of the air shock front through the duct is included in each plot. For the transient inflow cases, the broken line is the approximate path of the inflow at the peak pressure (delayed by 0.28 ms) condition. The boundary-layer parameters in Fig. 11 indicate establishment for the steady inflow case of about three to four flow times (G_s = 3–4) after shock passage. For the transient case the establishment times are about the same, but relative to the peak pressure line, only about two flow times.

The establishment times of the fuel mixing parameters are given in Fig. 12. The dotted line from the shock path at x = 0.114 m to the duct exit represents the path of the fuel jet, with a constant injection velocity of 2420 m/s. Two characteristic time scales are given, one based on the arrival of the initial shock (airflow velocity) and one on the fuel jet velocity. Both scales are measured from the flow arrival time at the duct exit. For the steady inflow case the mass flow ratio becomes established as the fuel jet is re-established. The mixing parameters (η, ϕ) require about one characteristic time after the jet flow reaches the duct exit. With transient inflow the mixing parameter establishes in about three characteristic times after the jet flow has re-established. The normalized equiv-

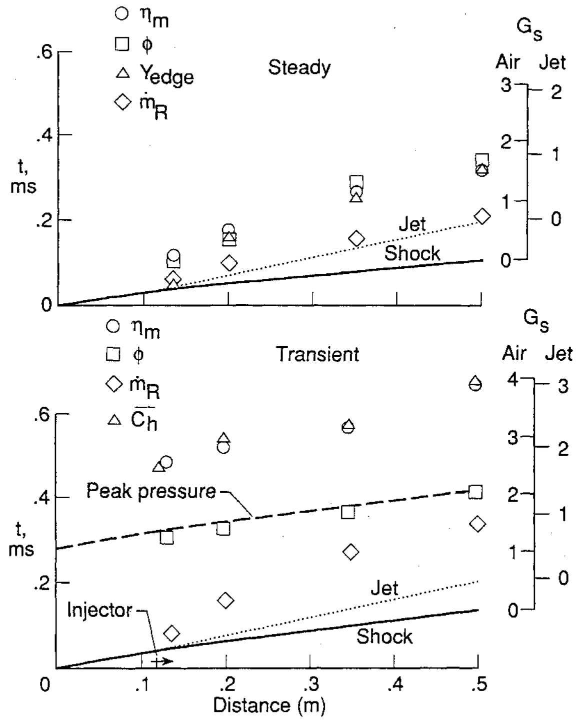

Fig. 12 Establishment times for fuel mixing parameters.

alence ratio sets up along the path of the peak air mass flow (dashed line). The airflow rate has a value of about 2 on the $(G_s)_{air}$ scale. The result of these comparisons is that the integral flow mixing parameters establish at least as fast as those dominated by viscosity. Since wall heat flux is commonly used in experimental facilities to indicate flow establishment, these results indicate that the mixing will also be established. If the flow is transient, care must be taken in normalization of the data to derive quasisteady values.

Concluding Remarks

A numerical simulation of the temporally developing flow through a generic scramjet combustor duct is presented for stagnation conditions typical of Mach 13 flight as produced by a shock tunnel pulse facility. The particular focus is to examine the startup transients and to determine the time required for certain flow parameters to become established. Calculations were made with a Navier-Stokes solver SPARK with temporally relaxing inflow conditions of velocity, pressure, and temperature derived from actual facility operation of the T4 shock tunnel at the University of Queensland in Australia. Calculations at nominal steady inflow conditions were made for comparison. The generic combustor geometry included the injection of hydrogen fuel from the base of a centrally located strut which was set to operate at steady state. In both cases the flow as assumed laminar and fuel combustion was not considered. Establishment times were determined for viscous parameters—boundary-layer and displacement thicknesses, wall shear, and heat flux, and for fuel-mixing parameters—fuel core length, fuel plume location, equivalency ratio, and mixing efficiency.

The principal results are estimates of the establishment times. Generally, the parameter history was examined and establishment taken as the time the parameter was within a certain increment of a steady-state value. Results for the steady inflow case are more consistent with accepted values with the boundary-layer parameters requiring about three to four characteristic times, and the mixing parameters about two characteristic times. For the transient inflow case the parameters did not (always) reach a steady value, in which case, the establishment time was taken to be indicated by the approach to a near-constant rate of change. Such a definition gave values that appear consistent when referenced to the passage of the peak conditions of the transient inflow. The results clearly show that the mixing parameters establish as fast as viscous parameters like heat flux, which is used to indicate flow establishment in experiments.

References

[1]Stalker, R. J., "Hypervelocity Aerodynamics with Chemical Nonequilibrium," *Annual Review of Fluid Mechanics*, Vol. 21, 1989, pp. 37–60.

[2]Morgan, R. G., et al., "Shock Tunnel Studies of Scramjet Phenomena," NASA CR-181721, Sept. 1988.

[3]Casey, R., and Stalker, R. J, et al., "Shock Tunnel Studies of Scramjet Phenomena—Supplement 5," NASA CR-182096, Oct. 1990.

[4]Tamagno, J., Bakos, R. J., and Pulsonetti, M. V., "Results of Preliminary Calibration Tests in the GASL HYPULSE Facility-Expansion Tube," GASL TR 308, Ronkonkomam, NY, May 1989.

[5]Tamagno, J., Bakos, R. J., and Pulsonetti, M. V., "Hypervelocity Real Gas Capabilities of GASL's Expansion Tube HYPULSE Facility," AIAA 16th Aerodynamic Ground Testing Conf., AIAA Paper 90-1390, June 1990.

[6]Hornung, H., and Sturtevant, B., "Challenges for High-Enthalpy Gasdynamic Research During the 1990's: Plans for the GALCIT T5 Laboratory," GALCIT Paper FM 90-1, Pasadena, CA, Jan. 1990.

[7]Jacobs, P. A., Rogers, R. C., Weidner, E. H., and Bittner, R. D., "Flow Establishment in a Generic Scramjet Combustor," AIAA/SAE/ASME/ASEE 26th Joint Propulsion Conf., AIAA Paper 90-2096, Orlando, FL, July 1990.

[8]Anderson, J. D., *Hypersonic and High Temperature Gas Dynamics*, McGraw-Hill, New York, 1989.

[9]Drummond, J. P., Rogers, R. C., and Hussainni, M. Y., "A Detailed Numerical Model of a Supersonic Reacting Mixing Layer," AIAA/ASME/SAE/ASEE 22nd Joint Propulsion Conf., AIAA Paper 86-1427, Huntsville, AL, June 1986.

[10]Drummond, J. P., "A Two-Dimensional Numerical Simulation of a Supersonic, Chemically Reacting Mixing Layer," NASA Langley Research Center, NASA TM-4055, Hampton, VA, Dec. 1988.

[11]Drummond, J. P., Carpenter, M. H., Riggins, D. W., and Adams, M. S., "Mixing Enhancement in a Supersonic Combustor," AIAA/ASME/SAE/ASEE 25th Joint Propulsion Conf., AIAA Paper 89-2794, Monterey, CA, July 1989.

[12]Roberts, G. O., "Computational Meshes for Boundary Layer Problems," *Lecture Notes in Physics*, Vol. 8, Springer-Verlag, London, 1971, pp. 170–177.